SUSPENDED NANOCHANNEL RESONATORS AT ATTOGRAM PRECISION

Selim Olcum[1], Nathan Cermak[1], Steven C. Wasserman[1], Kris Payer[1], Wenjiang Shen[2], Jungchul Lee[3], and Scott R. Manalis[1]

[1] Massachusetts Institute of Technology, Cambridge, MA, 02139 USA

[2] Innovative Micro Technology, Santa Barbara, CA, 93117 USA

[3] Sogang University, Seoul 121-742 Republic of Korea

ABSTRACT

Nanomechanical resonators can quantify individual particles down to a single atom; however the applications are limited due to their degraded performance in solution. Suspended micro- and nanochannel resonators can achieve vacuum level performances for samples in solution since the target analyte flows through an integrated channel within the resonator. Here we report on a new generation suspended nanochannel resonator (SNR) that operates at approximately 2 MHz with quality factors between 10,000-20,000. The SNR is measured to have a mass sensitivity of 8.2 mHz/attogram. With an optimized oscillator system, we show that the resonator can be oscillated with a mass equivalent frequency stability of 0.85 attogram (4 parts-per-billion) at 1 kHz bandwidth, which is 1.8 times the calculated stability imposed by the thermal noise. We demonstrate the use of this mass resolution by quantifying the mass and concentration of nanoparticles down to 10 nm in solution.

INTRODUCTION

Established nanoparticle characterization methods in solution are limited for diameters below about 50 nm, particularly for heterogeneous samples. Nanomechanical resonators can detect masses as low as single atoms due to their very small sizes and high quality factors. However their performance degrades dramatically in solution because of the fluid loading. Suspended micro- and nanochannel resonators (SMRs and SNRs) [1], [2] have opened up the possibility of achieving high-Q mass sensing in the aqueous environment by integrating a fluidic channel inside a cantilever. Previously, the performance of nanomechanical resonators in vacuum has been studied extensively. However, SNRs received only theoretical approaches so far [3] to study their limits of detection. Previously as a proof of concept for nanoparticle detection, SNRs achieved a limit of detection higher than 100 attograms at 1 kHz bandwidth [2], far above the limit imposed by the thermal noise at room temperature.

Here we report on the device and system level advancements that have enabled the mass equivalent stability down to 0.85 attogram at 1 kHz, which is 1.8 times the calculated thermomechanical noise limit. We first discuss the resonator and oscillator design and demonstrate an analysis on the stability of the developed system. Finally, we demonstrate the use of this mass resolution by measuring the mass and concentration of nanoparticles down to 10 nm in solution.

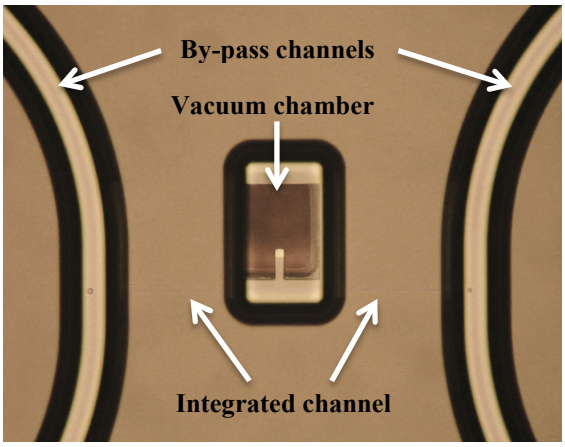

Figure 1: *A micrograph of the fabricated SNR. The cantilever, which is seen in the vacuum cavity, is 27 microns in length. Larger microfluidic channels at the sides are the by-pass channels for delivering and discarding the sample. 1 μm wide integrated channel, which is difficult to see in this micrograph, runs between the by-pass channels.*

RESONATOR DESIGN

The mass resolution of a mechanical mass sensor improves with higher mass sensitivity and/or better frequency stability. The mass sensitivity increases with increased resonant frequency and decreased resonator mass. For achieving sub-attogram level precision, we designed (Table 1) and fabricated (Fig. 1) 8-fold more sensitive cantilevers to changes in mass than the previous designs [2].

SNRs are manufactured by a previously described micro-fabrication process [2]. The process enables the cantilevers to vibrate in a vacuum cavity. Quality factors up to 20,000 are measured on the fabricated devices. An on-chip getter maintains the vacuum environment required for high-Q operation. There are four fluidic ports drilled on the top glass wafer to access the two bypass channels (50 μm X 20 μm) separated 285 μm apart at each side of the cantilever (Fig. 1). The U-shaped channel in the cantilever is connected to these bigger bypass channels by 140 μm-long channels with the same cross-section that is in the cantilever.

OSCILLATOR DESIGN

SNRs are operated in self-oscillation mode in a positive feedback loop. The oscillator consists of a photodetector as the vibration detector, a FPGA for phase shifting and signal processing and a piezo-ceramic for actuation.

Table 1: *Design dimensions and theoretically calculated properties of SNRs. Properties were calculated assuming the cantilevers are filled with water.*

Type	Length (μm)	Thickness (μm)	Width (μm)	Channel Height (nm)	Channel Width (μm)	Resonant Frequency (MHz)	Stiffness (N/m)	Mass (pg)	Sensitivity (mHz/ag)
SNR in [2]	50	1.3	10	700	2	0.76	7.4	1328	- 1.19
new SNR	27	1	7.5	400	1	1.99	16.9	443	-9.3

We implemented an optical lever setup for detecting the cantilever vibration. The vibration of the cantilever causes the angle of the cantilever tip to change, which is converted to the deflection of a laser beam bounced off of the tip. We used an ultra-low noise diode lab laser module (Coherent 635 nm, 5 mW) as the laser source. We implemented a spatial filter (0.5NA, 13.86 mm aspherical lens, 20 μm pinhole) to clean the laser beam. The beam is then collimated using a spherical lens (f = 30 mm) to achieve a ~3 mm-diameter filtered laser beam. For tuning the laser power hitting the cantilever, we used a film polarizer on a rotational stage at the output of the spatial filter since excessive laser power increases the frequency noise of the cantilever in closed loop operation. We focused the laser on the cantilever tip using a 20X objective (Nikon LU Plan ELWD 0.4NA). The reflected laser beam is then focused on a custom-made photodetector by an achromatic doublet lens (Thorlabs AC254-30-A).

For achieving the best signal-to-noise ratio we used a fast, split photo-diode (Hamamatsu S4204) as the photodetector with ultra-low-noise transimpedance amplifiers (OPA847) with 5 MHz 3 dB-bandwidth. The differential optical signals from the two channels of the split photodiode are converted to a single-ended voltage signal using a high speed instrumentation amplifier (AD8130). Finally, an automatic gain control (AGC) stage maintains a fixed amplitude at the output, which can be tuned by a DC input voltage.

The noise of the optical lever and photodetector system is dominated by the intrinsic thermomechanical fluctuations

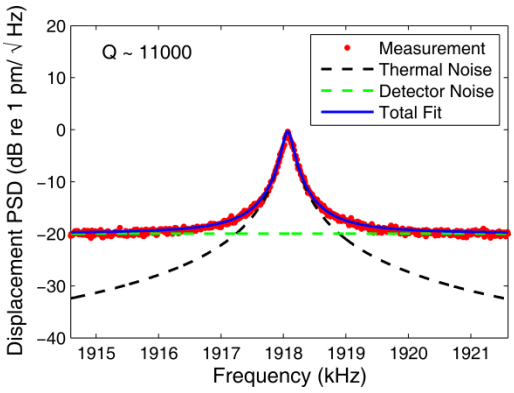

Figure 2: *Displacement noise density of a SNR due to thermal noise. The red circles are the spectrum analyzer measurements; the black line is the theoretical thermal noise and the green line is the photodetector noise (100 fm/Hz$^{1/2}$).*

of the cantilever around its resonant frequency (Fig. 2). The voltage noise power spectrum density of the photodetector output, S_V^{pd}(V^2/Hz) is measured using a spectrum analyzer (HP4395A) when the only driving force on a water-filled cantilever is generated by the thermal noise due to the room temperature, T (~300 K). To convert the measured voltage spectrum density to displacement noise spectral density, S_x^{th}, we used the derivation given in [4]:

$$S_x^{th}(\omega) = \frac{4\omega_0^3 k_B T}{kQ} \frac{1}{(\omega_0^2 - \omega^2)^2 + (\omega\omega_0/Q)^2} \quad (1)$$

where, k_B, k, Q and ω_0 are Boltzmann constant and stiffness, quality factor and resonant frequency of the cantilever. We can use (1) evaluated at the resonant frequency ($4k_BTQ/\omega_0 k$) to calculate the responsivity (V/m) of the vibration detection as follows:

$$R = \sqrt{\frac{S_V^{pd}(\omega_0) - S_V^{pd}(\omega \neq \omega_0)}{4k_BTQ/\omega_0 k}} \quad (2)$$

The quality factor and the resonant frequency is obtained by an open loop frequency scan. The stiffness is calculated by using the measured mass sensitivity of the cantilever using:

$$\frac{\delta f}{\delta m} = -\frac{f_0}{2m^*} = -\frac{2\pi^2 f_0^3}{k} \quad (3)$$

where $m^*$is the effective mass of the cantilever. Measured displacement power spectral density of a SNR is given in Fig. 2**.** The red circles are the spectrum analyzer measurements referred to displacement domain performed at 3 Hz resolution bandwidth with 100 averages. The dashed black curve is calculated using equation (1) and the dashed green line is the noise density of the photodetector referred to the displacement domain. We measured the detection noise floor as 100 $fm/\sqrt{Hz}$. It is seen in Fig. 2 that the noise at the photodetector output is dominated by the thermomechanical vibrations of the cantilever at the vicinity of its resonant frequency and by the detection noise floor at frequencies away from the resonant frequency.

The detected vibration signal at the output of the photodetector circuit is digitized (14 bits Terasic AD/DA at 100 MSPS) and passed to a FPGA (Altera Cyclone IV on DE2-115). The optimal delay required in the loop for stable self-oscillation is controlled by the FPGA with sub-clock precision (39 ps) using numerical interpolation. The FPGA and the conversion board run on an external 100 MHz oven controlled crystal oscillator clock (Abracon AOCJY2-E-H1C). The delayed signal is then converted back to analog by the conversion board to be used by the motion actuator.

To operate and oscillator with the best frequency stability, the amplitude of oscillation should be increased

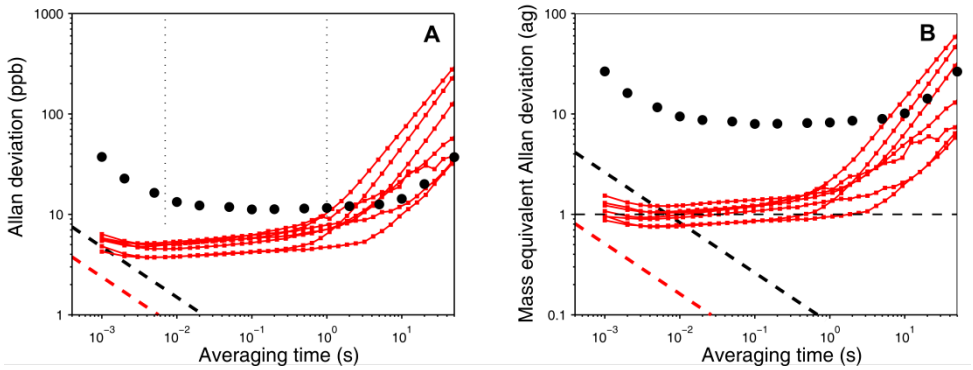

***Figure 3: A**. Allan deviation is plotted as a function of averaging (gate) time for new generation SNRs (red) and for previous studies [2] (black). Ultimate noise limits imposed by thermal energy at room temperature are shown as colored dashed lines. **B**, Mass precision of SNRs, defined as the mass equivalent Allan deviation.*

until Duffing type mechanical nonlinearity is observed [5]. For achieving high mechanical actuation amplitudes at 2 MHz, we used a single layer, hard piezo-ceramic (APC841, 7x7x0.2 mm) integrated underneath the SNR chip. The piezo-ceramic is driven by an amplifier utilizing a high current opamp (LT1210) output stage.

The frequency of oscillation is measured by period counting at 100 MHz using a digital heterodyne mixer and a low-pass filter coded in the FPGA. The input signal is mixed with a reference sinusoid generated by a numerically-controlled oscillator (NCO). The heterodyned signal is then filtered by a low pass filter and subsequently up-sampled (1^{st}-order hold) back to 100 MHz. The period of oscillation is then determined by counting the clock ticks between the zero-crossings of the filtered signal.

The oscillator setup is controlled by a control computer which communicates with the FPGA through the Ethernet. The frequency measurements is monitored by the computer and recorded for post-processing.

OSCILLATOR STABILITY

To access the frequency stability of the fabricated SNRs in closed loop, we calculated the Allan deviation of the measured oscillation frequency as a function of averaging time, when the cantilevers were filled with water. The measured frequency stability (red dots in Fig. 3A) ranges from 4 to 7 parts-per-billion at room temperature (without temperature control) using measurement bandwidths of 5-1,000 Hz. The red curves in Fig. 3A correspond to various tested SNR chips. Compared to the previous studies (black dots) the stability of the oscillator system is improved 10-fold at 1 kHz. When converted to mass (Fig. 3B) using the mass sensitivities given in Table 1, the improvement is more than 30-fold, which translates to a stability better than 1 attogram (10^{-21} kg) at 1 kHz.

To investigate the potential for further improvements in the stability and the mass precision, we calculated the ultimate limit of frequency stability imposed by the thermal energy due to room temperature. The power spectral density of the phase fluctuations of the oscillation, $S_\varphi^{th}(\omega)$, is calculated using the power spectral density of the random displacements of the cantilever due to thermal noise, $S_x^{th}(\omega)$, which was given in (1) as follows:

$$S_\varphi^{th}(\omega) = \frac{S_x^{th}(\omega)}{\langle x_c \rangle^2} \qquad (4)$$

For very high Q oscillators and as a function of the baseband modulation frequency, $\omega_m = \omega - \omega_0$, (4) can be approximated [4] as:

$$S_\varphi^{th}(\omega_m) \approx \frac{\omega_0 k_B T}{k \langle x_c \rangle^2 Q} \frac{1}{\omega_m^2} \qquad (5)$$

The Allan variance of the oscillation frequency due to the phase noise density is calculated as given in [6]:

$$\sigma_A^2(\tau) = 2\left(\frac{2}{\omega_0 \tau}\right)^2 \int_0^\infty S_\varphi(\omega)\, sin^4(\omega\tau/2)\, d\omega \qquad (6)$$

where τ is the averaging duration. If we evaluate the above integral using the phase noise density in (5), we get:

$$\sigma_A^{th}(\tau) = \sqrt{\frac{\pi k_B T}{\tau\, k \langle x_c \rangle^2\, Q\, \omega_0}} \qquad (7)$$

The SNRs used in this work are driven at their onsets of nonlinearity. Therefore we use the following approximate displacement expression of a cantilever given by Arlett et. al. [3] converted to RMS at the onset of nonlinearity in (7).

$$\langle x_c \rangle = 5.46 \frac{L}{\sqrt{2Q}} \qquad (8)$$

where L is the length of the cantilever. So the thermal noise limited Allan deviation at the onset of nonlinearity is:

$$\sigma_{A,non}^{th}(\tau) = \frac{1}{5.46L} \sqrt{\frac{k_B T}{\tau\, k\, f_0}} \qquad (9)$$

which is independent of the quality factor. Therefore, as long as an oscillator is driven at its onset of nonlinearity, the lowest Allan deviation that can be achieved does not depend on the quality factor of the cantilever. The ultimate limit of stability for SNRs is calculated and plotted in Fig. 3A and B using the same color codes. Measured frequency stability values at 1 ms averaging time are 1.8- to 3-fold (5-10 dB) above the thermomechanical noise limits.

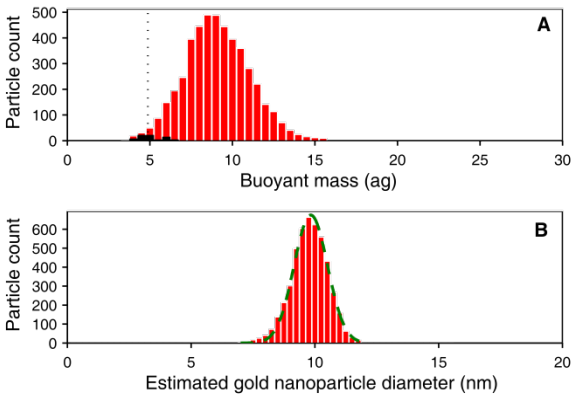

Figure 4: ***A****, Buoyant mass histogram (red) of 4,700 particles detected during a 70-minute experiment using a population of 10 nm gold nanoparticles in DI water.* ***B****, Diameter histogram is calculated assuming the particles are spheres of density 19.3 g/cm^3.*

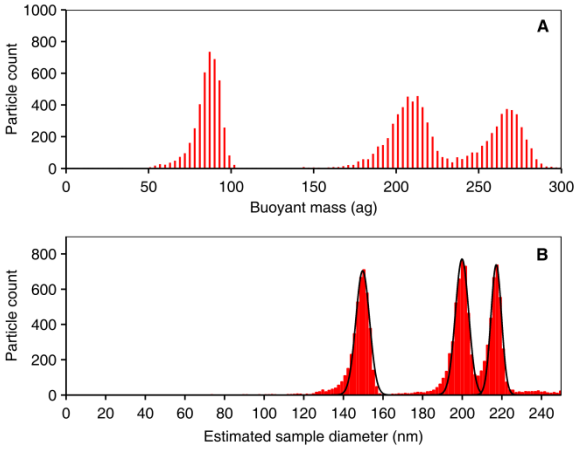

Figure 5: ***A,*** *Buoyant mass histogram of more than 12,500 detected particles in less than 30 minutes in a mixture of 150 nm, 200 nm and 220 nm polystyrene beads.* ***B,*** *Diameter histogram calculated assuming particles are spheres of density 1.05 g/cm^3.*

NANOPARTICLE ANALYSIS

The mass distribution and absolute particle concentration are important measures for analyzing nanoparticle populations. We sought to demonstrate the mass resolution of our system using size-calibrated 10 nm gold nanoparticles (NIST RM-8011). Before analyzing the sample, we calibrated the mass sensitivity (Hertz/gram) of the employed cantilever using size-calibrated 30 nm gold nanoparticles (NIST RM-8012), which are approximately 25 times heavier than the 10 nm particles. We determined that the mass sensitivity of the cantilever used is 8.2 mHz/ag slightly lower than the expected calculation. In a 70-minute experiment on 10 nm gold suspension, we measured 4,700 individual particles. Our results show a distinct population (Fig. 4A) around 9 attograms. The overlaid black histogram includes the detected peaks during a measurement with the same duration but without the particles as a control. We then estimated the diameter of each nanoparticle (Fig. 4B), assuming each particle is spherical and equally dense (the density of gold is 19.3 g/cm^3). The estimated mean size is 9.83 nm with a coefficient of variance of 6.9%, which agrees well with the manufacturer specification of 9.9 nm. The detection and estimation algorithm used can successfully estimate the transit time of a particle. The transit time information combined with the dimensions of the buried microfluidic channel enables the calculation of the particle concentration. We estimate the concentration of the nanoparticles as 1.95×10^9 particles/ml compared to the concentration of 1.90×10^9 particles/ml calculated using the information in the datasheet.

We also tested the dynamic range of the SNRs by weighing larger particles (150 nm, 200 nm and 220 nm polystyrene beads) using the same operation, detection and estimation conditions. The resulting mass histograms are given in Fig. 5 indicating the detection of each sub-population in the mixture successfully.

OUTLOOK

The range of buoyant mass that can only be reached by this new generation of SNRs includes many of the engineered nanoparticles used in nanomedicine, most of the virions like HIV, HCV, and natural sub-cellular structures such as exosomes. We envision this device will be useful for accurately analyzing nanoparticles in solution for a wide range of fields

REFERENCES

[1] T. P. Burg, M. Godin, S. M. Knudsen, W. Shen, G. Carlson, J. S. Foster, K. Babcock, and S. R. Manalis, "Weighing of biomolecules, single cells and single nanoparticles in fluid," *Nature*, vol. 446, no. 7139, pp. 1066–1069, Apr. 2007.

[2] J. Lee, W. Shen, K. Payer, T. P. Burg, and S. R. Manalis, "Toward Attogram Mass Measurements in Solution with Suspended Nanochannel Resonators," *Nano Lett.*, vol. 10, no. 7, pp. 2537–2542, Jul. 2010.

[3] J. L. Arlett and M. L. Roukes, "Ultimate and practical limits of fluid-based mass detection with suspended microchannel resonators," *J. Appl. Phys.*, vol. 108, no. 8, Oct. 2010.

[4] T. R. Albrecht, P. Grütter, D. Horne, and D. Rugar, "Frequency modulation detection using high-Q cantilevers for enhanced force microscope sensitivity," *J. Appl. Phys.*, vol. 69, no. 2, pp. 668–673, Jan. 1991.

[5] D. Greywall, B. Yurke, P. Busch, A. Pargellis, and R. Willett, "Evading Amplifier Noise in Nonlinear Oscillators," *Phys. Rev. Lett.*, vol. 72, no. 19, pp. 2992–2995, May 1994.

[6] A. N. Cleland and M. L. Roukes, "Noise processes in nanomechanical resonators," *J. Appl. Phys.*, vol. 92, no. 5, pp. 2758–2769, Sep. 2002.